

# Modeling and Simulation of Phonon Boundary Scattering in PDE-based Device Simulators

O. Tornblad<sup>1</sup>, P. G. Sverdrup<sup>2</sup>, D. Yergeau<sup>1</sup>, Z. Yu<sup>1</sup>, K. E. Goodson<sup>2</sup> and R.W. Dutton<sup>1</sup>

1) Center for Integrated Systems, Stanford University, Stanford, CA 94305-4075, USA, olof@gloworm.stanford.edu

2) Thermosciences Division, Mechanical Engineering, Stanford University, CA 94305, USA

**Abstract** - In this work, the effect of phonon boundary scattering on the heat transfer in thin silicon layers and close to interfaces was investigated. The modeling is applicable to Silicon-On-Insulator (SOI) devices as well as to conventional bulk technology. From a linearized Boltzmann Transport Equation (BTE), anisotropic local thermal conductivities are derived. A separate expression is formulated for the case of a bulk device where only one interface is present. Anisotropy was implemented as a finite element-based operator into the PROPHET device simulator and a demonstration of the new electrothermal modeling was made for a conventional MOSFET. The anisotropic local thermal conductivities lead to a temperature increase ~ 30 % higher at the gate oxide interface compared to conventional modeling.

## I. INTRODUCTION

Electrothermal modeling is important for accurate simulation of a number of semiconductor devices. Scaling has progressed to a state where characteristic lengths of the device are comparable to the phonon mean free path (approximately 300 nm at room temperature and 35 nm near the melting point of silicon [1,2]). Microscale heat transfer effects therefore need to be taken into account for simulation of deep submicron devices. When the thickness of a thin semiconducting layer approaches the phonon mean free path, scattering at the boundaries influences the thermal conductivity, see Fig. 1. Sondheimer [3] developed an expression for the effective electrical conductivity along thin metal layers, which is in good agreement with experimental data; using an average value for the conductivity works well for this case. In analogy, one might consider using an average value for the thermal conduc-

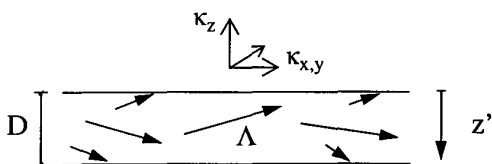


**FIG. 1** Heat transfer along a thin layer.  $\kappa_{x,y}$  denote the thermal conductivity along the film,  $\kappa_z$  the thermal conductivity across the film,  $D$  the thickness of the film and  $\Lambda$  the phonon mean free path.  $z'$  denotes the normalized position within the layer.

tivity in thin Silicon-On-Insulator (SOI) MOSFETs. However, in an electronic device, the electrical and thermal systems are coupled and a more refined description might be necessary. In the case of a bulk MOSFET, the need for a local description of the thermal conductivities close to the gate oxide is obvious. In this study, anisotropic local thermal conductivities are derived that can be used with the conventional heat flow equation. The new electrothermal modeling is demonstrated by simulation of a conventional MOSFET.

## II. THEORY

In the work by Sondheimer, an analytical solution for the effective electrical conductivity along a thin film is derived from a linearized form of the Boltzmann Transport Equation (BTE). Noting that the same derivation holds for phonon transport, a position-dependent local thermal conductivity can be identified as

$$\kappa_{x,y}(z') = \int_0^{\pi/2} \sin^3 \theta \left( 1 - e^{-\frac{D}{2\Lambda \cos \theta}} \cosh\left(\frac{D-2z'}{2\Lambda \cos \theta}\right) \right) d\theta \quad (1)$$

Here,  $D$  denotes the thickness of the film,  $\Lambda$  the phonon mean free path and  $z'$  the normalized position within the layer, see Fig. 1. The derivation assumes diffuse scattering at the interfaces, i.e. phonons scatter with the same probability in all directions. Sondheimer also worked out an expression taking partly specular reflection into account; this was not considered in this study but the extension is straightforward.

Following the same techniques as in [3], an expression can be derived for heat transfer across the layer and one arrives at

$$\kappa_z(z') = \int_0^{\pi/2} \sin \theta \cos^2 \theta \left( 1 - e^{-\frac{D}{2\Lambda \cos \theta}} \cosh\left(\frac{D-2z'}{2\Lambda \cos \theta}\right) \right) d\theta \quad (2)$$

These thermal conductivities can now be used with the conventional heat flow equation. For the ease of use and efficient

calculation in device simulators, these expressions were fitted with analytical functions that take the following form:

$$\kappa_{x,y}(z') = 1 - \frac{1}{2}e^{-\left(\frac{z'}{z_{char}}\right)^{\frac{3}{4}}} - \frac{1}{2}e^{-\left(\frac{1-z'}{z_{char}}\right)^{\frac{3}{4}}} \quad (3)$$

$$z_{char} = 0.32 \cdot 1/\delta; \quad \delta = D/\Lambda$$

$$\kappa_z(z') = 1 - \frac{1}{2}e^{-\left(\frac{z'}{z_{char}}\right)^{0.95}} - \frac{1}{2}e^{-\left(\frac{1-z'}{z_{char}}\right)^{0.95}} \quad (4)$$

$$z_{char} = 0.72 \cdot 1/\delta; \quad \delta = D/\Lambda$$

Fig. 2 shows the agreement between the analytical expressions and the fitting functions for three different ratios of film thickness to phonon mean free path  $\delta = D/\Lambda = 1, 3, 5$ . Note that the thermal conductivity across the layer is always lower than along the layer.

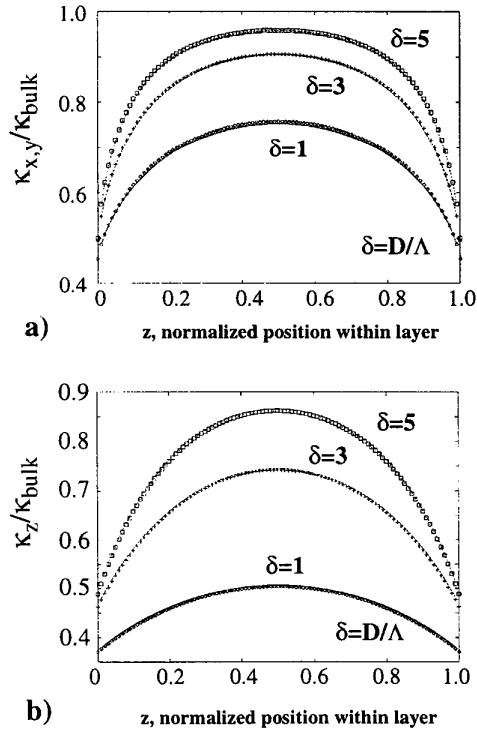


**FIG. 2** Local thermal conductivities as a function of position within a thin layer.  $\delta$  denotes the ratio of film thickness to the phonon mean free path. Solid lines denote fitting functions and symbols denote analytical solution from linearized BTE. a) along layer and b) across layer.

For a bulk case, the third terms in eq. (3) and (4) can be dropped (assuming the interface is located at  $z=0$ ) and the normalized position  $z'$  is converted to an absolute position  $z$ . This leads to the following expressions:

$$\kappa_{x,y}(z) = 1 - \frac{1}{2}e^{-\left(\frac{z}{0.32\Lambda}\right)^{\frac{3}{4}}} \quad (5)$$

$$\kappa_z(z) = 1 - \frac{1}{2}e^{-\left(\frac{z}{0.72\Lambda}\right)^{0.95}} \quad (6)$$

In Fig. 3, these conductivities are plotted as a function of distance from the interface for Si at  $T=300$  K ( $\Lambda=300$  nm was used for the phonon mean free path [1,2]).

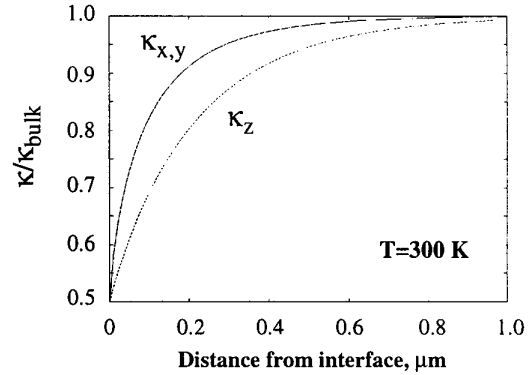


**FIG. 3** Anisotropic local thermal conductivities for bulk technology case where only one interface is of importance.

### III. NUMERICAL IMPLEMENTATION

The anisotropic thermal conductivity was implemented in PROPHET [4], a TCAD simulation platform that permits script-level specification of models as Partial Differential Equations (PDEs) that are built from reusable operators. In PROPHET, a user specifies each term in an equation at a high level as a combination of a discretized geometric operator (e.g. a finite element discretization for divergence) and a physical operator, which for divergence would represent the expression for the flux.

For example, the term “div  $k$  grad  $T$ ” in the equation for  $T$  with a scalar, but potentially spatially varying  $k$ , could be represented in a PROPHET script as:

$$\text{termN} = \text{fel\_div.diffusion}(k, T|T) \quad (7)$$

where  $\text{fel\_div}$  is the finite element divergence geometric operator,  $\text{diffusion}$  is a diffusive flux physical operator, the  $k$  and  $T$  before the  $|$  are the input variables and the  $T$  after the  $|$  is the equation to which this term is being applied.

In the case of the anisotropic conductivity, a new physical operator that treats  $k$  as a tensor needed to be implemented. For this work, only the diagonal components of the tensor are needed. Thus, the new physical operator only needs three input variables for the conductivity and can be specified as

$$\text{termN} = \text{fel\_div.aniso\_kappa}(k_x, k_y, k_z, T|T) \quad (8)$$

The actual analytical expressions in eq. (3)-(6) are directly defined as spatially varying fields by the user in the simulation input deck.

In linking the geometric and physical operators together at the native code level, PROPHET has powerful mechanisms for tensor manipulation. Hence, the implementation of the new  $\text{aniso\_kappa}$  physical operator based on the existing diffusion operator involves little effort (in fact, a change of only three lines of code for the core numerical computation). This case illustrates the advantages of the well thought out abstractions and modular structure in the PROPHET platform.

#### IV. SIMULATION

To demonstrate the effect of the new electrothermal modeling, a conventional MOSFET was simulated under static conditions. Fig. 4 shows a schematic of the structure (not drawn to scale). The structure is used for demonstration purposes only and does not correspond to state-of-the-art technology or any device in production. The breakdown voltage is  $V_{ds} \sim 8.5$  V at  $V_{gs} = 0$  V and the snapback voltage at  $V_{gs} = 2.5$  V is  $> 5$  V. Thermal electrodes coincide with the electrical contacts for source, drain and backside and are tied to 300 K; heat flow in the gate oxide was not taken into account. The channel length is  $\sim 0.9$   $\mu\text{m}$  and source-drain junction depths are  $\sim 0.15$   $\mu\text{m}$ . The thermal conductivity for the bulk Si material was set to 148.4 W/m·K; the temperature dependence of the thermal conductivity was not included at this point.

The heat generation term in the heat flow equation was represented by Joule heat ( $\mathbf{J} \cdot \mathbf{E}$ ), which should be a very good approximation for a MOSFET operating under normal static conditions (i.e. no large effects of carrier recombination,

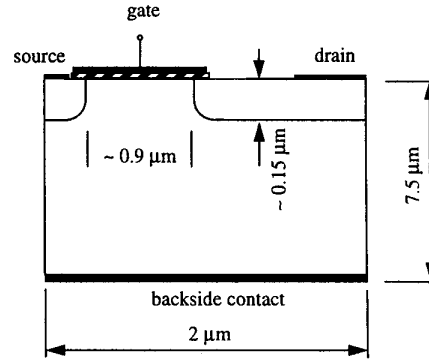


FIG. 4 Schematic of simulated MOSFET.

impact ionization, heterojunctions or transient terms [5]). The Joule heat peaks at the drain side close to the gate oxide where the product of electric field and current is higher. The operating conditions were  $V_{ds} = 4.5$  V and  $V_{gs} = 2.5$  V, corresponding to a drain current of  $5.3 \cdot 10^{-4}$  A/ $\mu\text{m}$ . Fig. 5 shows the temperature distribution in the structure including anisotropic local thermal conductivities compared to a reference case with conventional bulk thermal conductivity. Temperature distributions are plotted along cutlines  $y = 0$   $\mu\text{m}$  and  $x = 1$   $\mu\text{m}$ . The difference in temperature rise is approximately 30 % in the hottest region.

#### V. DISCUSSION

The importance of the boundary scattering on the heat transfer in a MOSFET is intimately related to the location and size of the heat source. For a pronounced effect, the heat source needs to be located very close to the interface and its size in the vertical direction must be comparable to the characteristic lengths for the anisotropic thermal conductivities (see Fig. 3). This depends on the device design and possibly also on operating conditions. The effect might be slightly larger in a transient case. Pure thermal simulations typically yielded a maximum difference of  $\sim 50$  % in temperature rise between the new and conventional modeling for a small heat source. For state-of-the-art SOI-technology, the thickness of the silicon layer is on the order of 50 nm. This translates to  $\delta = D/\Lambda \sim 0.17$  and the effect of boundary scattering is going to be very important for this case. However, the variation of thermal conductivity within the layer is not large. As can be seen in Fig. 2, already at  $\delta = 1$ , the variation over the layer is not dramatic. Averaged values for the thermal conductivities along and perpendicular to the layer can then be used to a very good approximation. For thicker layers or higher temperatures the situation might be different.

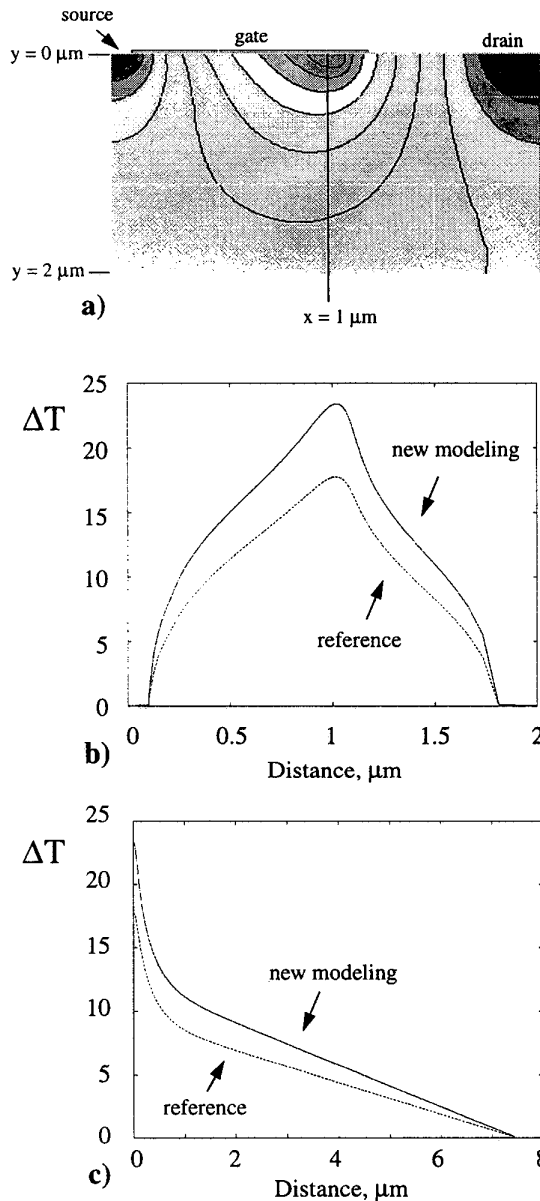


FIG. 5 Temperature distributions from electrothermal simulations using PROPHET for a bulk MOSFET during static conditions; a) temperature map for electrothermal simulation including new modeling. b) comparison of temperature distributions for new and conventional modeling along cutline  $y = 0 \mu\text{m}$ . c) same as b) but along  $x = 1 \mu\text{m}$ .

## VI. CONCLUSIONS

In this work, the effect of phonon boundary scattering on the heat transfer in thin silicon layers and close to interfaces was investigated. Anisotropic local thermal conductivities were derived from a linearized Boltzmann Transport Equation. A separate expression was formulated for the case of a bulk device where only one interface is present. Anisotropy was implemented as a finite element-based operator into the PROPHET device simulator and a demonstration of the new electrothermal modeling was made for a conventional MOSFET. The temperature increase at the gate oxide interface was  $\sim 30\%$  higher with the anisotropic local thermal conductivities compared to conventional modeling.

## ACKNOWLEDGMENTS

O. Tornblad thanks the following organizations for fellowships utilized during 1999 in the initial part of this work: Wennergren Foundations, Ericsson, Sydkraft and Frans Georg and Gull Liljenroths foundation.

## REFERENCES

- [1] Y. S. Ju and K. E. Goodson, "Impact of Phonon Dispersion upon the Size Effect on Thermal Conduction along Thin Semiconductor Films", Proc. ASME, Dallas, TX, DSC-Vol. 62, pp. 181-190, 1997.
- [2] P. G. Sverdrup, Y. S. Ju and K. E. Goodson, "Sub-Continuum Simulations of Heat Conduction in Silicon-On-Insulator Transistors", Proc. ASME IMECE, Nashville, TN, HTD-Vol. 364-3, pp. 41-49, 1999.
- [3] E. H. Sondheimer, "The Mean Free Path of Electrons in Metals", Advances in Physics, Vol. 1, no. 1, Jan. 1952.
- [4] C. S. Rafferty, Z. Yu, B. Biegel, M. G. Ancona, J. Bude, and R. W. Dutton, "Multi-dimensional quantum effect simulation using a density-gradient model and script-level programming techniques", SISPAD '98, p. 137, Leuven, Belgium, Sept. 1998.
- [5] O. Tornblad, U. Lindefelt and B. Breitholtz, "Heat generation in bipolar semiconductor devices: the relative importance of various contributions", Solid-State Electronics, Vol. 39, pp. 1463-1471, 1996.